0026-895X/94/040627-12$03.00/0

MOLECULAR PHARMACOLOGY, 46:627–638, 1994.

Rhodamine Efflux Patterns Predict P-glycoprotein Substrates in the National Cancer Institute Drug Screen

JONG-SEOK LEE, KEN PAULL, MANUEL ALVAREZ, CURTIS HOSE, ANNE MONKS, MIKE GREVER, ANTONIO TITO FOJO, and SUSAN E. BATES

Medicine Branch, Clinical Oncology Program (J.-S.L., M.A., A.T.F., S.E.B.), and Information Technology, Developmental Therapeutic Program (K.P., M.G.), Division of Cancer Treatment, National Cancer Institute, National Institutes of Health, Bethesda, Maryland 20892, and Program Resources, Inc./DynCorp, National Cancer Institute, Frederick Cancer Research and Development Center, Frederick, Maryland 21702 (C.H., A.M.)

Received February 15, 1994; Accepted July 6, 1994

SUMMARY

Fifty-eight cell lines in the National Cancer Institute drug screen were analyzed for their ability to efflux the fluorescent dye rhodamine 123 as a functional assay for P-glycoprotein (Pgp). Using flow cytometry, the rhodamine fluorescence was measured for each cell line under four incubation conditions, i.e., after accumulation in the presence or absence of the Pgp antagonist cyclosporin A and after efflux in rhodamine-free medium in the presence or absence of cyclosporin A. The results in some cell lines were compatible with Pgp-mediated efflux. There was a significant correlation between *mdr*-1 expression and rhodamine efflux in the 58 cell lines ($r = 0.788$, $p = 0.0001$). Using the rhodamine efflux data as a seed for COMPARE analysis with the cytotoxicity data on >30,000 compounds in the National Cancer Institute drug screen database, hundreds of compounds with high correlation coefficients were identified. Selected compounds were tested for reversal of cross-resistance in a multidrug-resistant cell line. A high degree of reversibility, up to 10,000-fold, for some of the compounds was noted in the presence of the Pgp antagonist PSC 833. This finding suggested that compounds with predominately Pgp-mediated resistance were being identified. Using these compounds as seeds for COMPARE analysis against a more restricted database of 187 standard agents, a series of standard compounds were repeatedly identified as having high correlation coefficients with the newly identified Pgp substrates. These standard agents, including phyllanthoside, bisantrene, and homoharringtonine, constitute an *mdr*-1 profile. New agents identified as being highly correlated with these compounds may benefit from clinical trials with Pgp antagonists.

The goal of the drug evaluation program of the NCI is to discover new anticancer agents through large-scale, semiautomated screening of compounds in human tumor cell lines. To achieve the goal of new drug discovery, approximately 10,000 compounds are screened yearly, by cytotoxicity assay, using 60 human tumor cell lines in disease-oriented panels (1). More than 30,000 compounds have been screened using this approach and a number of agents have been readied for clinical trial. Data from the cytotoxicity assays are stored in the COMPARE database. The differing sensitivities of the 60 cell lines allow a unique profile, termed a fingerprint, to be generated for each compound when the IC_{50} values are plotted on a graph. Using the drug sensitivity data, the COMPARE analysis program computes correlation coefficients that describe the degree of similarity of two compounds (2, 3). It has been reported that compounds with similar mechanisms of action, such as those binding tubulin, have similar profiles and high correlation coefficients (4, 5). In contrast, compounds with unique mechanisms of action have unique profiles and may be identified as potentially useful anticancer agents. One important question for interpreting these results is how important a role various mechanisms of drug resistance play in influencing the outcome for each compound.

Pgp, which has been widely described as providing a mechanism for MDR, has been shown to confer both acquired and intrinsic resistance to cells in the laboratory, although its role in clinical drug resistance is still under investigation (6–8). Pgp confers MDR by active efflux of chemotherapeutic agents out of the cell. A surface membrane glycoprotein of 170 kDa encoded by the *mdr*-1 gene, Pgp appears to require substrate binding before transport. Although the requirements for binding and transport have not been clearly identified, a wide range of compounds have been described to be transported by Pgp.

Rhodamine 123 is a fluorescent dye that was observed in early studies to accumulate in mitochondria to variable degrees, depending on the cell type (9, 10). Rhodamine was initially considered a potential anticancer agent because it was more cytotoxic to carcinoma cells than to normal epithelial cells (11,

ABBREVIATIONS: NCI, National Cancer Institute; Pgp, P-glycoprotein; FCS, fetal calf serum; MDR, multidrug resistance; SDS, sodium dodecyl sulfate; SSC, standard saline citrate; MRP, multidrug resistance-associated protein; CsA, cyclosporin A; PCR, polymerase chain reaction; GI_{50}, 50% growth inhibitory concentration.

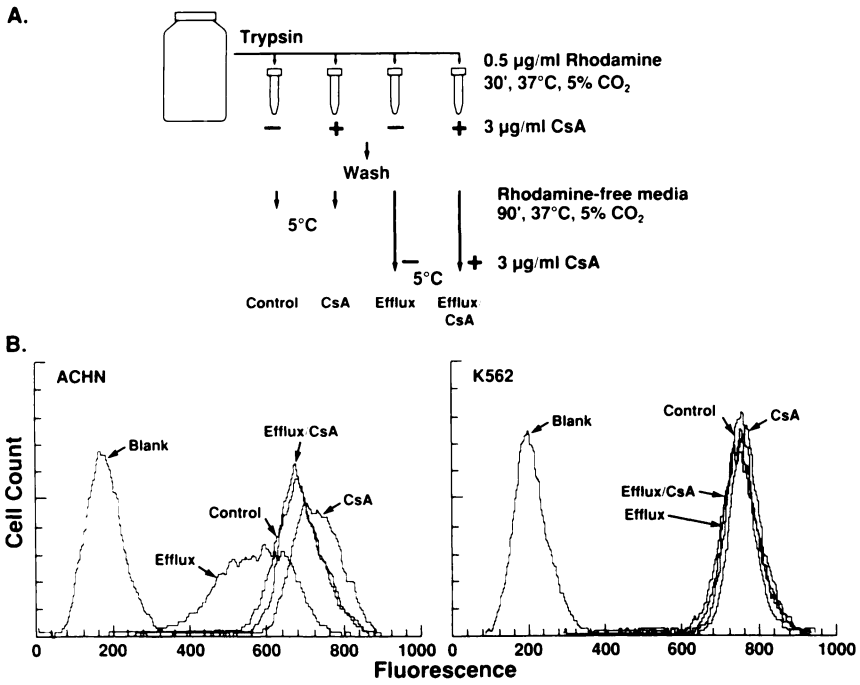

Fig. 1. Rhodamine accumulation and efflux assay in the cell lines of the NCI drug screen. A, Schematic diagram demonstrating rhodamine accumulation [in the absence (*Control*) or presence (*CsA*) of 3 µg/ml CsA] and efflux [in the absence (*Efflux*) or presence (*Efflux/CsA*) of 3 µg/ml CsA] periods. B, Representative histograms for two cell lines, i.e., ACHN, a Pgp-expressing kidney carcinoma line, and K562, a non-Pgp-expressing leukemia line. Cells were incubated continuously in the presence or absence of CsA.

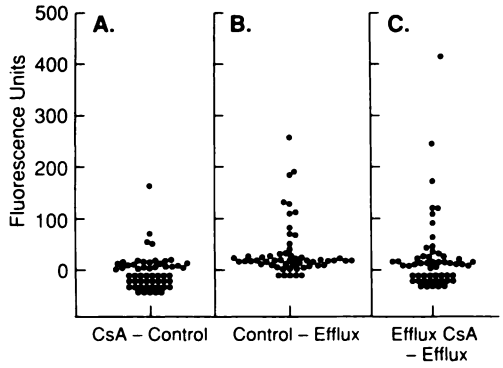

Fig. 2. Scatter plot of calculated differences in rhodamine accumulation measured by flow cytometry under three conditions. A, Plot of the difference in accumulation due to the addition of the Pgp antagonist CsA. B, Plot of the difference in fluorescence after the accumulation phase and after the efflux phase in the absence of CsA. C, Plot of the difference in fluorescence in the cells after efflux in the presence or absence of CsA. This gave the greatest difference in the results.

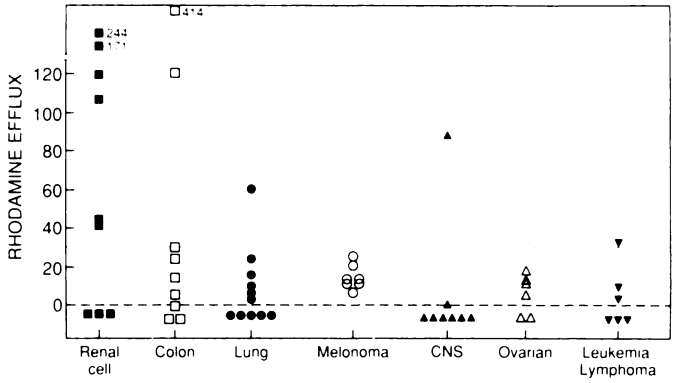

Fig. 3. Rhodamine efflux values in the 60 cell lines of the NCI drug screen. The cell line panel is tumor specific, with cell lines derived from kidney, colon, lung, central nervous system (*CNS*), and ovarian cancers and from leukemia or lymphoma. The calculated difference in channel number for rhodamine efflux in the presence and absence of CsA is shown. *Dashed line*, cells with no efflux; negative values are found below that. *Solid line*, SW620 level of efflux (30 fluorescence units): the significance of efflux below this level is not known.

12). In retrospect it appears that the apparent selectivity was a result of Pgp expression in the normal kidney cells and its absence in the particular carcinoma cell lines studied, because multiple investigators have reported that rhodamine 123 is a substrate for Pgp (13–17). In addition, Pgp has been implicated as the mechanism underlying the ability of bone marrow stem cells to "exclude" rhodamine (16, 18). The natural fluorescence of rhodamine, like that of the anthracyclines, allows a nonradioactive method for determining Pgp function by flow cytometric analysis (19). Compared with the anthracyclines, quenching of fluorescence is not observed with rhodamine. Preliminary experiments in our laboratory confirmed the higher sensitivity of rhodamine efflux, compared with daunorubicin efflux, in identifying MDR cells.

Expression of *mdr*-1 has been determined in the 60 cell lines of the NCI drug screen.[1] This was done to determine which cell lines might have Pgp-mediated drug resistance and to learn whether the selection of active compounds identified by the screen was influenced by Pgp. Because the activity of Pgp can be modulated, the possibility remained that the levels of *mdr*-1 expression would not always correlate with the degree of efflux (20–23). We hypothesized that a functional assay for Pgp

[1] M. Alvarez, K. Paull, A. Monks, C. Hose, J. S. Lee, J. Weinstein, M. Grever, S. Bates, and T. Fojo. Expression of *mdr*-1/P-glycoprotein in the cell lines of the NCI anticancer drug screen program as a tool to identify novel P-glycoprotein substrates and antagonists. Submitted for publication.

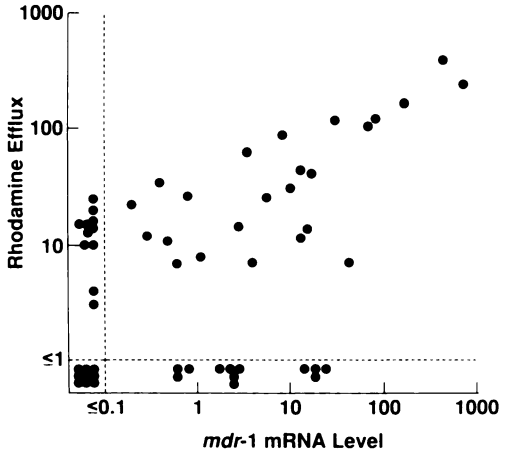

Fig. 4. Correlation of *mdr*-1 mRNA level with rhodamine efflux. Values for *mdr*-1 mRNA determined by PCR analysis are plotted on the *x*-axis; calculated rhodamine efflux is on the *y*-axis. The correlation between the two yields $r = 0.788$ ($p = 0.0001$).

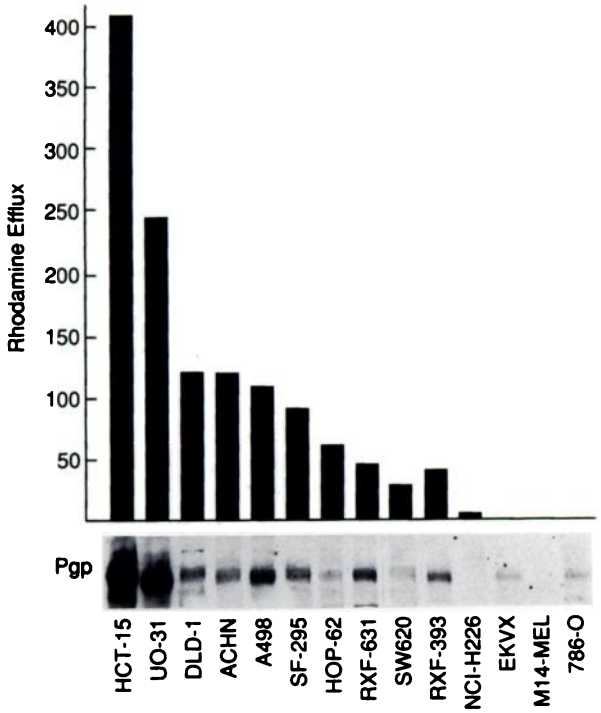

Fig. 5. Rhodamine efflux and Pgp expression in drug screen cell lines. *Lower*, the cell lines with significant efflux and those with discordance with the *mdr*-1 results were analyzed by immunoblotting. *Upper*, the calculated values for rhodamine efflux in the presence and absence of CsA are shown. Note that in two cell lines, EKVX and 786–0, Pgp is detectable by immunoblotting but is not accompanied by measurable rhodamine efflux.

could provide additional information for identifying Pgp substrates in the screen. We therefore undertook characterization of the rhodamine 123 efflux pattern for each of the cell lines of the NCI drug screen.

Materials and Methods

Cell lines. The 60 cell lines comprising the anticancer drug screen were obtained, evaluated, and characterized as described previously (1). All cell lines were adapted to growth in RPMI 1640 medium containing 5% FCS and 5 mM glutamine. The cells were expanded and cryopreserved to provide a continuous stock of cells to be replaced in the screen after every 20 passages. Fifty-eight of the 60 cell lines were available for the rhodamine assay; the remaining two were omitted due to aberrant growth and have been replaced in the screening panel. The cell lines were derived from the malignancies of patients either not treated or treated with radiation and/or chemotherapy. The cell lines represent leukemia, melanoma, and cancers of the lung, colon, brain, kidney, and ovary.

The multidrug resistant SW620 Ad300 subline was derived by stepwise exposure of human colon carcinoma SW620 cells to doxorubicin. This subline is maintained in 300 ng/ml doxorubicin and demonstrates a classical multidrug resistant phenotype, with broad cross-resistance, increased Pgp expression, decreased drug accumulation, and reversibility of the multidrug resistant phenotype by verapamil (24). The levels of *mdr*-1 mRNA expression in this cell line are 140-fold higher than those of parental SW620 cells.

Compounds. Compounds used for this study were obtained through the Drug Synthesis and Chemistry Branch, NCI (Bethesda, MD).

Rhodamine efflux assay. Suspensions of logarithmic phase cells were obtained from tissue culture plates by trypsinization. During the accumulation period, four aliquots of cells were resuspended in rhodamine-containing medium (Improved minimum essential medium with 10% FCS and 0.5 μg/ml rhodamine 123) and incubated with or without 3.0 μg/ml CsA at 37° in 5% CO_2 for 30 min. After the accumulation period, efflux was initiated by sedimention at 600 × *g* and resuspension in rhodamine-free medium (Improved minimum essential medium with 10% FCS), with or without 3.0 μg/ml CsA. The efflux was carried out at 37° in 5% CO_2 for 90 min. At the end of both the accumulation and efflux periods, cells were sedimented, washed in ice-cold Hanks' buffered salt solution, placed in Hanks' buffered salt solution with 10% FCS on ice, and kept in the dark until flow cytometric analysis. Samples were analyzed on a FACScan flow cytometer (Becton Dickinson) equipped with a 488-nm argon laser. The green fluorescence of rhodamine 123 was collected after a 530-nm band pass filter. Samples were gated on forward scatter versus side scatter to exclude cell debris and clumps. A minimum of 6000 events were collected for each sample.

Immunoblotting. Cells were harvested in 10 volumes of STM buffer (250 mM sucrose, 10 mM Tris·HCl, pH 7.5, 1.5 mM $MgCl_2$, 20 μg/ml aprotinin, 1.0 mM phenylmethylsulfonyl fluoride) and lysed with an ultrasonic homogenizer (25). Unbroken cells and cell nuclei were sedimented at 1000 × *g* for 5 min. Crude membrane fractions were then prepared by sedimentation at 100,000 × *g* for 30 min. The pellets were dissolved in STM buffer for protein determination (Bio-Rad) and repelleted. The pellets were dissolved in SDS sample loading buffer. Samples (50 μg) were subjected to SDS-polyacrylamide gel electrophoresis and electrophoretically transferred to nitrocellulose membranes overnight. The blots were blocked with 3% bovine serum albumin in TTBS (0.1% Tween 20, 20 mM Tris·HCl, pH 7.5, 150 mM NaCl) for 2 hr. The blots were then incubated for 1 hr with the primary antibody (1/2000 dilution of polyclonal antiserum 4007) (26). After being washed three times with TTBS, the blots were incubated for 1 hr with secondary antibody (1/2000 dilution of horseradish peroxidase-conjugated goat anti-rabbit IgG). After the blots were washed three times with TTBS, immunoreactive protein was detected using an enhanced chemiluminescence method (Amersham).

Northern analysis. Total RNA was extracted by homogenization in guanidium isothiocyanate, followed by centrifugation through a cesium chloride cushion. RNA was then separated on a 1% agarose/6% formaldehyde gel with 10 μg of RNA loaded in each lane. The gel was blotted to a nylon membrane by capillary transfer overnight. Transferred RNA was fixed to the nylon membrane with UV light (Stratagene UV linker). The blots were prehybridized for 1 hr at 58° in prehybridization solution (50% formamide, 6× SSC (standard saline citrate; SSC = 0.15 M NaCl, 0.015 M sodium citrate), 5× Denhardt's solution, 1.0% SDS, 100 μg/ml salmon sperm DNA). For hybridization, synthetic riboprobe was prepared by SP6 polymerase transcription

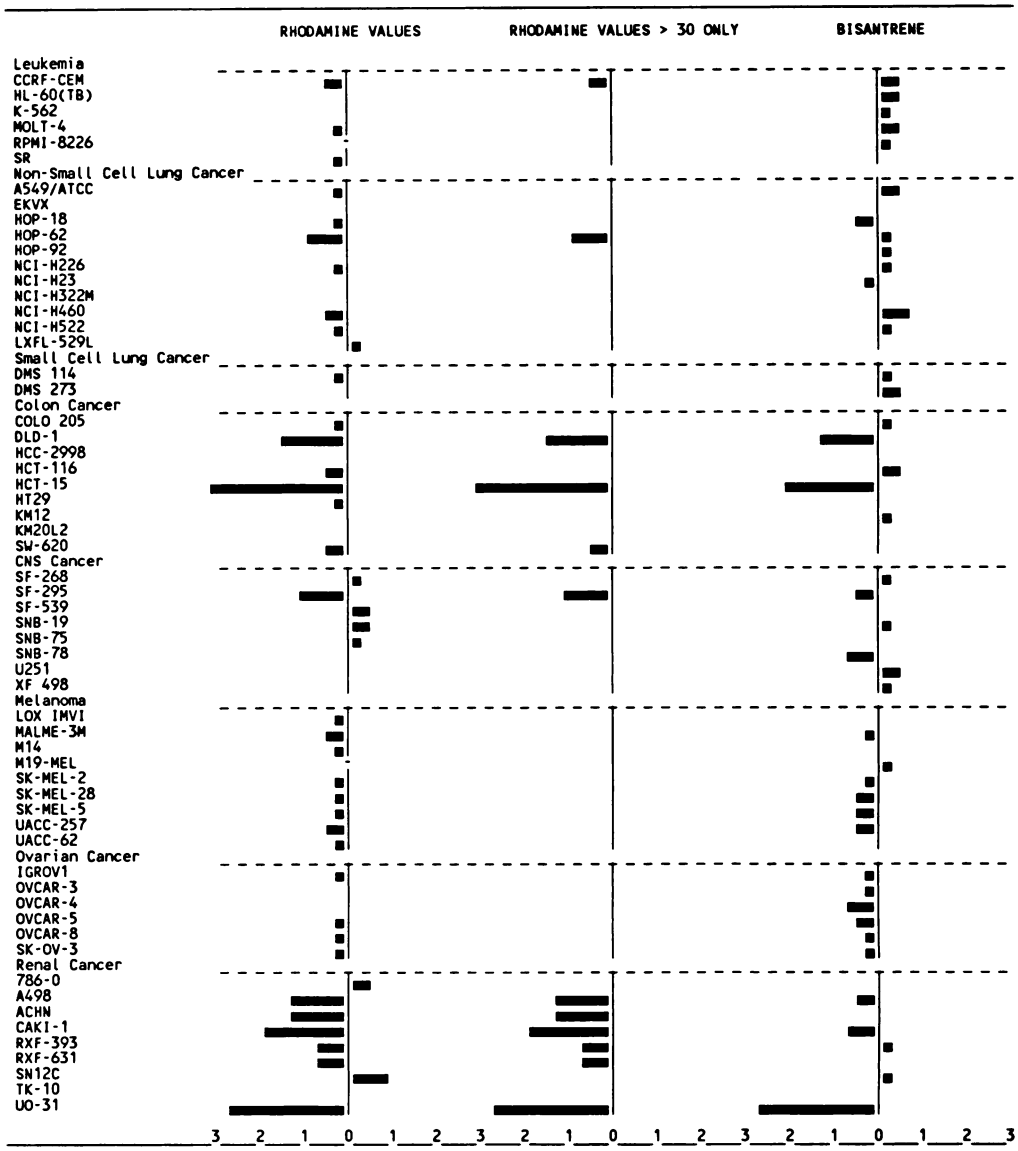

Fig. 6. Comparison of the simulated mean graph for rhodamine efflux with the mean graph for bisantrene. *Left*, the simulated mean graph was derived from the values obtained for rhodamine efflux in all 58 cell lines. *Middle*, a restricted pattern that includes the 12 cell lines with a rhodamine efflux value of >30 is shown. *Right*, this pattern can be compared with the mean graph of bisantrene, a compound with a high Pearson correlation coefficient (r = 0.835). Visual inspection demonstrates similarities between the ideal graph and that of bisantrene.

(Promega) using [^{32}P]UTP. A 1379-base pair cDNA containing sequences from the middle third of the *mdr*-1 gene (bases 1176–2555) was used as the template for riboprobe synthesis. Radiolabeled probe (2×10^6 cpm/ml) was added directly to the prehybridization buffer and the blots were hybridized at 58° for 12–18 hr. After hybridization, the blots were washed twice in 1× SSC/1.0% SDS at room temperature for 20 min, twice in 0.2× SSC/1.0% SDS at 68° for 20 min, and twice in 0.1× SSC/0.1% SDS at 68° for 20 min. The filters were exposed to Kodak XAR film at −70° using an intensifying screen.

PCR analysis of *mdr*-1 and MRP mRNA expression. Reverse transcription and 30 cycles of PCR were performed as described previously for *mdr*-1 (27)[1] and with the following modifications for MRP. The optimal annealing temperature was 60.8°, and the magnesium concentration was adjusted to 2.5 mM. The MRP upper primer (25-mer, 5′ position 793) was 5′-CGGAAACCATCCACGACCCTAATC-3′; the MRP lower primer (25-mer, 3′ position 1063) was 5′-ACCTCCTCATTCGCATCCACCTTG-3′. Samples were separated on a 2% NuSieve/1% agarose gel and quantitated by comparing ethidium bromide staining by densitometry.

***In vitro* cytotoxicity assay.** Cytotoxicity assays were performed in 96-well microtiter plates using the colorimetric method described by Skehan *et al.* (28). Cells were seeded in 96-well plates at a density of 1000 cells/well, in 100 μl of growth medium (RPMI 1640 medium with 10% FCS), and incubated at 37° in 5% CO_2. Cytotoxic agents, with or without Pgp modulators, were diluted in 100 μl of the growth medium and were added to the plate 24 hr after seeding. The cells were then incubated for 96 hr in 5% CO_2 at 37°. After the 96-hr exposure to cytotoxic agents (with or without modulators), cells were fixed by addition of 50 μl of 50% trichloroacetic acid. Trichloroacetic acid-fixed cells were stained for 30 min with 0.4% (w/v) sulforhodamine-B dissolved in 1% acetic acid. At the end of the staining period, sulforhodamine-B was removed and the wells were rinsed four times with 1% acetic acid to remove unbound dye. Bound dye was solubilized with 10 mM unbuffered Tris base, pH 10.5. The cell density was determined by measuring the absorbance at 564 nm.

COMPARE analysis. The version of COMPARE used in this work differs from the original version of COMPARE that made comparisons based on a calculated mean difference in "deltas" (2). The current

TABLE 1

Top 20 compounds and an additional 8 compounds among the top 100 identified by COMPARE, using rhodamine efflux data

NSC number	Pearson correlation coefficient	Chemical name
656735	0.976	
172946	0.972	
Discreet	0.957	
Discreet	0.945	
643004	0.934	
646605	0.929	
52947	0.928	
Discreet	0.927	
Discreet	0.926	
Discreet	0.917	
58514	0.916	Chromomycin A3
Discreet	0.916	
Discreet	0.915	
259969	0.913	Deoxybouvardin
131547	0.911	
630176	0.904	
177365	0.903	
Discreet	0.902	
328426	0.902	Phyllanthoside
38270	0.899	Olivomycin
259968	0.899	Bouvardin
260610	0.899	
110363	0.894	
381856	0.886	Trioxacarcin A
337766	0.835	Bisantrene HCl
325014	0.828	Bactobolin
3053	0.826	Actinomycin D
245398	0.816	

version of COMPARE is usually configured to calculate pairwise correlations with the negative logarithm of one of the specific NCI cell line activity parameters, i.e., GI_{50}, total growth inhibition (TGI), or 50% lethal concentration (LC_{50}) (3). For instance, the GI_{50} is the NCI designation for a time 0-corrected IC_{50}, the concentration of agent causing 50% growth inhibition. Thus, $-\log_{10}(GI_{50})$ values for a "seed" or probe compound are correlated with the corresponding data for each compound in a database containing data for hundreds or even tens of thousands of screened compounds. In this paper the GI_{50} data were utilized in the COMPARE studies and the seed data were derived from the rhodamine efflux assays, as described below. The correlation coefficients used are generally the Pearson correlation coefficients output by the SAS[2] procedure PROC CORR, using the out=outp option, but for this paper we also calculated Spearman correlation coefficients, using the out=outs option for PROC CORR, for those correlations employing a small subset of the available seed values. The Spearman correlations were investigated because of a concern that for these small subsets the seed data deviated too much from a normal distribution for the Pearson method to be used. In fact, the Spearman correlation coefficients differed little from the Pearson correlation coefficients.

This application of COMPARE differs from all previously reported applications of the algorithm in that the seed data are not generated from cell line screening data. Instead, the seed data are measurements of rhodamine efflux in each of the cell lines used in the NCI screen. The COMPARE database stores the screening data as $-\log_{10}(GI_{50})$ for historical reasons related to the mean graph sign conventions. This means that data from more drug-resistant cell lines are stored with smaller values than those of more drug-sensitive cell lines. Therefore, the negative of the rhodamine efflux measurements was actually used as the seed data. We hypothesized that, the larger the rhodamine efflux value for a particular cell line, the greater the Pgp-mediated drug resistance in that cell line. The highest positive correlation coefficients should be obtained with database compounds whose drug resistance was best correlated with Pgp-mediated resistance.

It might be argued that the transformation to $-\log_{10}(x)$ (where x is rhodamine efflux) makes good sense because the database is built from $-\log_{10}(GI_{50})$ values. The argument is not as logical as it might sound, but it was tested. The results did not appear better than when $-x$ was used. Thus, we used $-x$ for the seed values.

To make the operation of this special application of COMPARE more easily visualized, we invoked the paradigm of the mean graph (2). By constructing a mean graph of the rhodamine efflux seed values as $-x$, we can see a mean graph pattern that represents a perfect match (correlation coefficient = 1.0) in the COMPARE application described above. The best matches will be those database compounds with mean graphs best correlated with this idealized mean graph.

Results

Cells were subcultured in flasks and then trypsinized before incubation with rhodamine. Intracellular rhodamine fluorescence was measured by flow cytometric analysis. Both trypsinization and storage on ice were carefully tested and found not to interfere with the results. Cells were first incubated in rhodamine-containing medium, with or without 3 μg/ml CsA. After 30 min, one half of each incubation was washed and kept on ice in the dark until flow cytometric analysis. Data collected at this point constituted the accumulation results. The other half of each incubation was washed and resuspended in rhodamine-free medium for an efflux period continuing with or without CsA. Flow cytometric analysis performed after 90 min in rhodamine-free medium quantitated the amount of rhodamine remaining in the cells after the efflux period. Fig. 1 depicts typical histograms for a Pgp-expressing cell line and a non-Pgp-expressing cell line. Blank values to determine autofluorescence were obtained for all cell lines. Histograms of cells incubated during the accumulation phase in rhodamine-containing medium without or with CsA and incubated during the period of efflux in rhodamine-free medium without or with CsA are presented for comparison. Pgp-expressing cells such as ACHN demonstrated an increase in the accumulation of rhodamine in the presence of CsA, compared with control, a decrease in rhodamine after efflux in the absence of CsA, and an increase in rhodamine fluorescence in cells incubated with CsA during the efflux period. Little difference was observed under any of the conditions in K-562 cells, which do not express Pgp.

Histograms identical to those shown in Fig. 1 were generated for every cell line. The median rhodamine fluorescence obtained for each peak was identified by the channel number, and this number (denoting the logarithm of fluorescence intensity) was used to indicate the amount of rhodamine in the cells in each incubation condition. The differences between channel numbers for the four incubation conditions described above were calculated and are plotted in Fig. 2. A difference of 256 channel numbers represents a 10-fold change in fluorescence intensity. In some of the cell lines, the addition of CsA increased rhodamine accumulation (Fig. 2A). In these lines, rhodamine fluorescence also decreased after the period of efflux in rhodamine-free medium (Fig. 2B). In 10 of 21 cell lines without *mdr*-1 mRNA expression, rhodamine fluorescence increased after the efflux period. This was felt to be due to concentration of rhodamine in mitochondria during the efflux period. Thus, calculations that subtracted fluorescence values after efflux from those after accumulation were not suitable indices of Pgp

[2] SAS is a registered trademark of the SAS Institute (Cary, NC).

TABLE 2

COMPARE analysis of 176 standard agents, using rhodamine efflux data

COMPARE analysis of 176 standards agents, using rhodamine efflux data as the seed for the algorithm, was performed. The top 20 compounds are shown, along with important other agents drawn from the list.

NSC number	Pearson correlation coefficient	Spearman correlation coefficient	Chemical name
Top 20 standard agents			
328426	0.902	0.972	Phyllanthoside
337766	0.835	0.891	Bisantrene HCl
3053	0.835	0.797	Actinomycin D
49842	0.794	0.860	Vinblastine
125973	0.782	0.882	Paclitaxel
123127	0.764	0.650	Adriamycin
325014	0.755	0.685	Bactobolin
58514	0.417	0.683	Chromomycin A3
82151	0.746	0.699	Daunomycin
164011	0.744	0.636	Rubidazone
237020	0.736	0.697	Largomycin
157365	0.720	0.564	Neocarzinostatin
349174	0.693	0.685	Piroxantrone
141633	0.676	0.721	Homoharringtonine
305884	0.669	0.697	Acodazole HCl
267469	0.631	0.394	Deoxydoxorubicin
355644	0.601	0.491	Anthrapyrazole
139105	0.592	0.721	Soluble Baker's antifol
339004	0.586	0.697	Chloroquinoxaline sulfonamide
526417	0.574	0.683	Echinomycin
Important other agents			
141540	0.494	0.545	Etoposide
119875	0.474	0.427	Cisplatin
26271	0.287	0.196	Cyclophosphamide
63878	0.280	0.112	Cytosine arabinoside
8806	0.239	0.203	Melphalan
339555	0.206	0.181	Bryostatin
79037	0.159	0.371	Cyclohexylchloroethylnitrosourea
38721	0.041	−0.168	Mitotane
180973	−0.094	−0.140	Tamoxifen

activity. To minimize the effects of non-Pgp-mediated efflux and nonspecific changes in fluorescent intensity, we used the difference in fluorescence at the end of the efflux period between cells incubated with and without CsA as a measure of Pgp activity (Fig. 2C). The fluorescence intensity after efflux in the absence of CsA was subtracted from that after efflux in the presence of CsA. This value is referred to as the level of rhodamine efflux. In some cell lines without *mdr*-1 expression, rhodamine fluorescence decreased with the addition of CsA, resulting in a negative value. This was felt to be a nonspecific effect of CsA, and all negative values were considered to be 0.

The differences in fluorescence at the end of the efflux period were plotted and analyzed by cancer cell type. As shown in Fig. 3, colon and kidney cancer cells demonstrated the greatest difference. Three additional cell lines, derived from a lung cancer, a central nervous system tumor, and a leukemia, had large differences as well. However, a range of values was obtained, and it was unclear which value represented the lowest level of significant Pgp activity. To help guide this decision, we considered that SW620 cells have detectable *mdr*-1 expression and detectable Pgp and can be sensitized to vincristine 4–6-fold by verapamil (29). The level of rhodamine efflux observed in these cells was 31. Thus, levels of rhodamine efflux of >30 were considered to represent significant Pgp activity. Twelve cell lines, including SW620, demonstrated efflux levels of >30.

To compare *mdr*-1 expression with Pgp function, the rhodamine efflux values were plotted against *mdr*-1 mRNA values measured by PCR, using the quantitative PCR assay that we described previously (27). As shown in Fig. 4, there was a good overall correlation between rhodamine efflux and *mdr*-1 expression. Comparing all of the values, a Pearson correlation coefficient of 0.788 ($p = 0.0001$) was derived. Because in a few of the cell lines there was discordance between the level of rhodamine efflux and the level of *mdr*-1 expression measured by PCR, we evaluated the Pgp level by immunoblotting. As shown in Fig. 5, there was a good correlation between the Pgp level on the immunoblot and the degree of rhodamine efflux. Cell lines with *mdr*-1 expression without detectable rhodamine efflux had low or undetectable Pgp levels on the immunoblot. This suggests that the differences observed were more likely the result of a discordance between the mRNA and protein levels for *mdr*-1/Pgp than the result of a nonfunctional protein.

The possibility that the discordance is due to the presence of the MRP drug resistance protein was evaluated using available MRP data obtained by quantitative PCR assay (27, 30).[3] MRP levels ranged from 2.6 to 32.4, with SW620 cells again serving as a control with a level of 10. The average MRP level for cell lines with rhodamine efflux greater than 30 was 9.03 ± 4.3, whereas cell lines without detectable rhodamine efflux had an average MRP level of 15.9 ± 8.8. The four cell lines with rhodamine efflux above 10 and no *mdr*-1 expression had MRP values of 9.7, 6.1, 24.2, and 19.7. The three lines with rhodamine efflux above 30 and *mdr*-1 levels less than 10 had MRP levels of 10.8, 15.9, and 6.0. The data suggest that MRP expression

[3] A. T. Fojo, S. E. Bates, and M. Alvarez, unpublished observations.

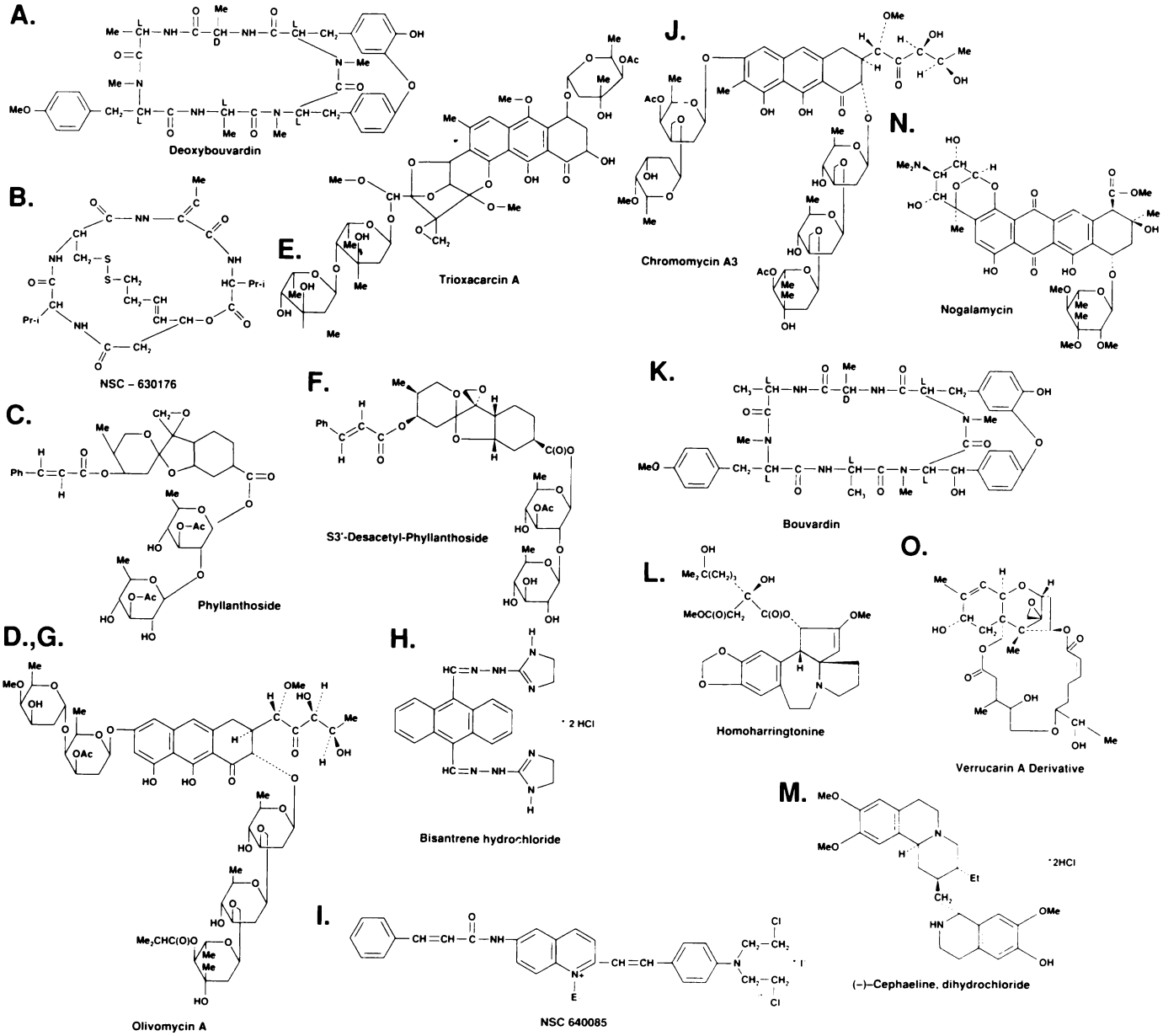

Fig. 7. Chemical structures of compounds with high Pearson correlation coefficients tested with Pgp modulators in Table 3. *Me*, methyl; *Ac*, acetyl; *Pr-i*, isopropyl; *Ph*, phenyl; *Et*, ethyl.

cannot explain the presence of rhodamine efflux in cells lacking *mdr*-1 mRNA.

We next asked whether the rhodamine efflux data could be used to identify Pgp substrates from the NCI drug screen. First, a profile was generated using the rhodamine efflux values, defined above as the difference between the efflux values in the presence and absence of CsA. This profile, or fingerprint, graphically depicts the rhodamine efflux values of all cell lines relative to each other. Then, using the COMPARE analysis, the drug screen database was searched for compounds with a cytotoxicity profile similar to the rhodamine efflux profile. Correlation coefficients were calculated for the relationship of the profile of each compound to the rhodamine efflux profile. Fig. 6 presents one example. In Fig. 6, the rhodamine efflux profiles of the 58 cell lines (Fig. 6, *left*) and of the 12 cell lines with values of >30 (Fig. 6, *middle*) are compared with the cytotoxicity profile of bisantrene (Fig. 6, *right*). A correlation coefficient of 0.835 was calculated when the rhodamine profiles of the 12 cell lines with values of >30 were compared with the bisantrene cytotoxicity profile for these 12 cell lines. Using a similar analysis, 100 compounds with correlation coefficients above 0.816 were identified; a large majority had not been previously recognized as Pgp substrates. COMPARE identified 282 and 999 compounds with correlation coefficients above 0.700 and 0.500, respectively. The only well known Pgp substrate present among the top 100 compounds was actinomycin D. Table 1 lists 30 compounds identified by this COMPARE analysis, including the top 20 plus an additional 8 in the top 100. These compounds include phyllanthoside, deoxybouvardin, bisantrene, chromomycin A3, bouvardin, and olivomycin. In addition, a restricted database of "standard" drugs, including conventional chemotherapeutic agents and others that have been studied in patients, was analyzed. This analysis demonstrated high correlation coefficients for vinblastine ($r = 0.793$),

TABLE 3
Cytotoxicity assays of putative PgP substrates in SW620 Ad300 cells

NSC number		Chemical name	r	IC_{50}	IC_{50} + PSC 833[a]	DMF,[b] PSC 833	IC_{50} + verapamil[c]	DMF, verapamil
				ng/ml	ng/ml		ng/ml	
49842		Vinblastine	0.793	57	0.16	356	0.9	63
125973		Paclitaxel	0.791	210	1.8	117	19	11
123127		Doxorubicin	0.764	1,400	5.8	241	26	54
757		Colchicine	0.684	90	1.6	56	19	5
141540		Etoposide	0.494	1,800	180	10	2,100	1
256439		Idarubicin	0.221	4.9	0.33	15	0.72	7
259969	A[d]	Deoxybouvardin	0.913	5,100	4	1,275	130	39
630176	B	Cyclic peptide derivative	0.904	1,400	0.4	3,500	21	67
328426	C	Phyllanthoside	0.902	1,800	2.1	857	65	28
76411	D	Olivomycin	0.886	24,000	2.3	10,435	46	522
381856	E	Trioxacarcin	0.886	210	0.52	404	15	14
342443	F	Desacetyl phyllanthoside	0.852	13,000	34	382	950	14
38270	G	Olivomycin	0.851	30,000	3.2	9,375	75	400
337766	H	Bisantrene	0.835	2,000	100	200	2,200	9
640085	I	Aniline mustard derivative	0.821	17,000	75	227	2,400	7
58514	J	Chromomycin A3	0.747	290	1.5	193	14	21
259968	K	Bouvardin	0.733	2,300	3.9	590	75	31
141633	L	Homoharringtonine	0.676	670	14	48	36	19
32944	M	Cephaeline di-HCl	0.600	120	2.9	41	2.9	41
70845	N	Nogalamycin	0.600	1,500	18	83	120	13
269754	O	Verrucarin A derivative	0.509	1,900	20	95	190	10

[a] PSC 833 was added at 1.5 μg/ml.
[b] DMF, dose modifying factor [DMF=IC_{50}/(IC_{50} + modifier)].
[c] Verapamil was added at 5 μg/ml.
[d] Letters refer to structure in Fig. 7.

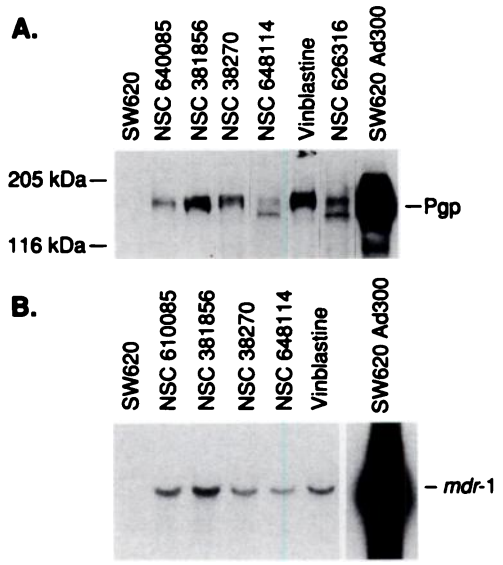

Fig. 8. Expression of Pgp and *mdr*-1 in SW620 sublines selected with putative Pgp substrates. A, Western blot analysis of protein harvested from parental SW620 cells and six sublines derived by selection with five potential Pgp substrates or vinblastine. For comparison, the result for SW620 Ad300 cells is shown. B, Expression of *mdr*-1 mRNA, detected by Northern blot analysis, in the same selected sublines.

paclitaxel (r = 0.791), and doxorubicin (r = 0.764), suggesting that Pgp substrates were indeed being identified (Table 2). Low correlation coefficients were obtained for compounds known to be more poorly transported by Pgp and also for drugs that are not Pgp substrates. Two compounds that block Pgp-mediated drug efflux had correlation coefficients of <0.1 (mitotane and tamoxifen) (31, 32).

An inspection was made of the structures of the compounds ranking in the top 100 places on the COMPARE list. Several considerations reduced this list to 90 compounds, e.g., if the compound appeared more than once because multiple concentration ranges existed in the COMPARE database or the compound had an undefined molecular weight or an undefined structure. These structures were then compared with all chemicals in the NCI chemical database. The putative Pgp substrates varied from the norm in several ways. At least 36 (41%) of the putative Pgp substrates were clearly of natural origin; this is estimated to be 10 times the percentage of purified natural products in the NCI chemical database. Several more compounds were semisynthetic in origin.

The molecular weight distribution of Pgp substrates also appeared unusual. The average molecular weight of 452,084 chemicals, with defined molecular weights, in the NCI chemical database is about 325. The molecular weights of the putative Pgp substrates appeared to be distributed differently, according to their net charge type. There were 48 neutral molecules (no ionized or ionizable groups at physiological pH), with an average molecular weight of 861 (2.6 times the NCI chemistry database average). A cationic charge or basic side chain (cationic at physiological pH) appeared in 40 of the 90 molecules, and these had an average molecular weight of 517 (1.6 times the NCI chemistry database average) but only 60% of the molecular weight average of neutral Pgp substrate molecules. There were only two anionic molecules, one a carboxylic acid with a molecular weight of 852 and the other a potassium polyoxometalate [$K_{12}(YPW_{30}O_{110})$], which is presumably polyanionic in aqueous solution, with a molecular weight of 7988. The chemical structures of 14 compounds subsequently confirmed to be Pgp substrates by reversal of resistance are shown in Fig. 7. The diversity of their structures is apparent.

To prove that the compounds with high correlation coefficients were indeed Pgp substrates, cytotoxicity assays were performed. We reasoned that Pgp substrates would have re-

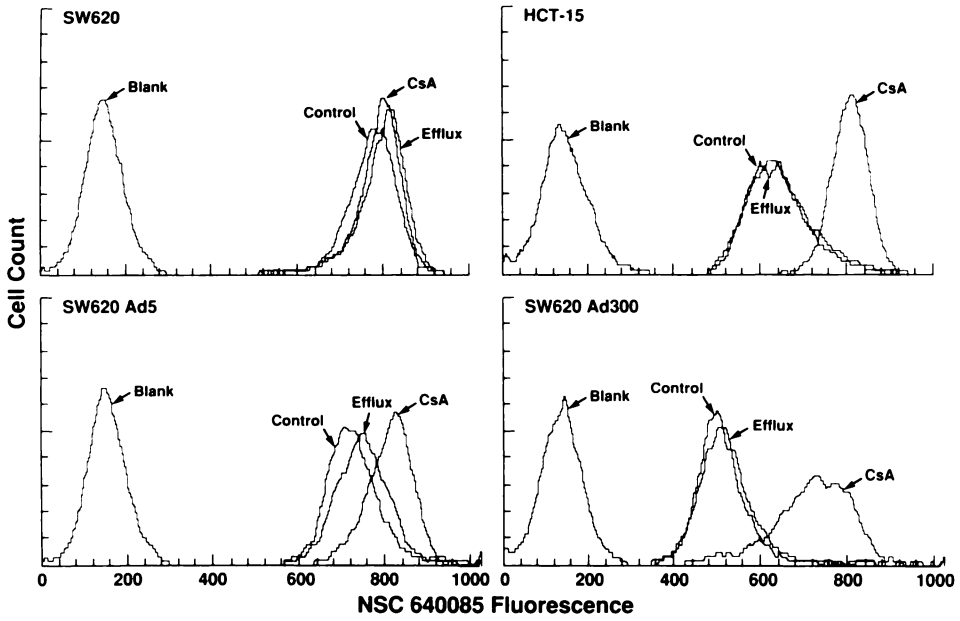

Fig. 9. Histograms of flow cytometric analysis of NSC 640085 fluorescence in multidrug resistance cells. Curves representing three conditions are shown for all four cell lines. Aliquots of cells were incubated with 1 μg/ml NSC 640085 for 1 hr in the presence or absence of CsA (3 μg/ml). At the end of the accumulation period one aliquot of control cells was placed in NSC 640085-free medium to allow for efflux for 90 min before flow cytometric analysis.

duced cytotoxicity in a multidrug resistant cell line. The degree of resistance reversal by Pgp antagonists would provide some indication of transport efficiency. Multidrug resistant SW620 Ad300 human colon carcinoma cells, selected for resistance to doxorubicin, were seeded in 96-well plates. The following day, cells were treated with increasing concentrations of the identified compounds, both in the absence and in the presence of the Pgp antagonists verapamil and PSC 833. Both 2.5 μg/ml verapamil and 1.5 μg/ml PSC 833 were minimally toxic to Ad300 cells. In every case, as shown in Table 3, the Pgp antagonists sensitized the cells to the cytotoxic compounds, providing evidence that these compounds were Pgp substrates.

Additional evidence that these compounds were Pgp substrates was obtained by inducing Pgp-mediated drug resistance after exposure of the cells to cytotoxic concentrations of the compounds. For these studies, parental SW620 cells were selected with vinblastine and each of five compounds showing high correlation coefficients. Selections were begun with 1–10 ng/ml drug and the concentrations were increased in a stepwise manner. RNA and protein were harvested from the selected sublines after culture for 2–3 months in the presence of increasing concentrations of drug. As shown in Fig. 8A, increased Pgp expression could be demonstrated in each of the sublines by immunoblotting. The levels of expression in the selected cells were comparable to those present in cells exposed to vinblastine for the same duration. In Fig. 8B, *mdr*-1 expression measured by Northern analysis is shown for five of the six selecting agents. Detectable *mdr*-1 levels were readily apparent, although at this early step in selection the levels were much lower than those observed in the multidrug resistant SW620 Ad300 cells. Taken together, these results support the conclusion that compounds with high correlation coefficients for rhodamine efflux are Pgp substrates.

Two final studies support this conclusion. One of the substrates identified by the COMPARE analysis was noted to be brightly colored and potentially fluorescent. Parental SW620 and HCT-15 cells and multidrug resistant SW620 Ad5 and Ad300 cells were incubated with this compound, treated with CsA, allowed to efflux, and then subjected to flow cytometric analysis. As shown in Fig. 9, decreased accumulation of NSC 640085 was observed in multidrug resistant SW620 Ad300 cells, relative to parental SW620 cells. Efflux was not observed, but increased accumulation was observed after treatment with the Pgp antagonist CsA in both HCT-15 and SW620 Ad300 cells. This result is consistent with Pgp-mediated transport of NSC 640085 in multidrug resistant cells.

During evaluation of the specificity of the results of the COMPARE analysis, three top compounds identified as Pgp substrates in Table 1 and confirmed in Table 4 were used as seeds for the COMPARE algorithm, using the standard agent database. Data from all 60 cell lines were included. Each Pgp substrate was highly correlated with several agents also found among the top 20 identified in Table 2 when rhodamine was used as the seed for the standard agent database. The same eight standard agents repeatedly sorted to the top, having the highest correlation coefficients among the 187 standard agents (Table 4, A-C). These eight compounds, including phyllanthoside, bisantrene, paclitaxel, Adriamycin, chromomycin A3, rubidazone, homoharringtonine, and deoxydoxorubicin, constitute an "MDR profile." When new agents are tested in the drug screen, a COMPARE analysis is performed, using the new agent as a seed against the standard agent database. If the MDR profile results, that new compound can be identified as a Pgp substrate (Table 4, D and E).

Discussion

In the present study, the accumulation and efflux of rhodamine were determined in 58 of the 60 cell lines of the new drug

TABLE 4
COMPARE analysis of Pgp substrates in the standard agent database

NSC number	Pearson correlation coefficient	Chemical name
A. Seed: deoxybouvardin		
337766	0.899	Bisantrene HCl
58514	0.877	Chromomycin A3
328426	0.872	Phyllanthoside
267469	0.771	Deoxydoxorubicin
141633	0.702	Homoharringtonine
3053	0.658	Actinomycin D
165563	0.653	Bruceantin
164011	0.653	Rubidazone
125973	0.634	Paclitaxel
123127	0.633	Adriamycin
49842	0.625	Vinblastine sulfate
B. Seed: NSC 630176		
337766	0.798	Bisantrene HCl
328426	0.743	Phyllanthoside
3053	0.600	Actinomycin D
267469	0.587	Deoxydoxorubicin
49842	0.584	Vinblastine sulfate
58514	0.529	Chromomycin A3
330500	0.521	Macbecin II
123127	0.505	Adriamycin
141633	0.485	Homoharringtonine
164011	0.477	Rubidazone
125973	0.472	Paclitaxel
C. Seed: olivomycin		
337766	0.846	Bisantrene HCl
58514	0.844	Chromomycin A3
267469	0.834	Deoxydoxorubicin
328426	0.812	Phyllanthoside
165563	0.731	Bruceantin
164011	0.689	Rubidazone
141633	0.687	Homoharringtonine
305884	0.681	Acodazole HCl
24559	0.678	Mithramycin
123127	0.658	Adriamycin
125973	0.638	Paclitaxel
D. Seed: NSC 656734		
328426	0.803	Phyllanthoside
337766	0.678	Bisantrene HCl
3053	0.599	Actinomycin D
58514	0.555	Chromomycin A3
141633	0.551	Homoharringtonine
267469	0.520	Deoxydoxorubicin
164011	0.516	Rubidazone
123127	0.511	Adriamycin
165563	0.510	Bruceantin
325014	0.493	Bactobolin
349174	0.468	Oxanthrazole (piroxantrone)
E. Seed: NSC 659852		
328426	0.898	Phyllanthoside
337766	0.830	Bisantrene HCl
141633	0.753	Homoharringtonine
3053	0.698	Actinomycin D
49842	0.683	Vinblastine sulfate
125973	0.665	Paclitaxel
58514	0.658	Chromomycin A3
164011	0.624	Rubidazone
139105	0.617	Soluble Baker's antifol
123127	0.616	Bruceantin
165563	0.609	Macbecin II

screen of the NCI.[4] Rhodamine efflux, calculated as the difference between the efflux values obtained in the presence and in the absence of CsA, was used as a measure of the functional activity of Pgp in the cell lines. Significant rhodamine efflux, defined as a difference in the efflux values of >30, was found in 12 cell lines; nine of these were colon or kidney cell lines. There was good overall concordance between measurement of rhodamine efflux and *mdr*-1 expression. The Pearson correlation coefficient for *mdr*-1 expression and rhodamine efflux for all 58 cell lines was 0.788, with a p value of < 0.0001. A good correlation between expression of Pgp, as measured by immunoblotting, and rhodamine efflux was also observed in a subset of the cell lines. The expression of MRP mRNA has also been measured in the 58 cell lines (30).[5] With SW620 cells being assigned a level of 10, MRP levels ranged from 2.6 to 36.4 and showed no correlation with rhodamine efflux ($r = -0.23$). MRP levels were comparable in cell lines with or without rhodamine efflux. The data suggest that MRP could not account for rhodamine efflux in lines with low *mdr*-1 expression.

The COMPARE computer program was utilized to search the NCI database for compounds with cytotoxicity profiles similar to the rhodamine efflux profile.[6] Hundreds of compounds were identified, many of them natural products. A fraction of these compounds were tested and shown to be Pgp substrates by reversal of resistance with verapamil or PSC833 and by the increased *mdr*-1/Pgp expression observed in cells exposed to the compounds. For some compounds, cytotoxicity could be modulated several thousandfold by Pgp antagonists. These results expand the list of known Pgp substrates and indicate that some "supersubstrates" may have their activity markedly enhanced by Pgp antagonists. The results also allow the identification of an MDR profile to identify new compounds in the screen as Pgp substrates.

The identification by COMPARE analysis of hundreds of compounds with high correlation coefficients for rhodamine efflux indicates a broad "substrate specificity" of Pgp. This suggests that transport by Pgp is a frequent occurrence for natural products, providing more support for the hypothesis that Pgp has a physiological role in healthy cells, to export naturally derived toxins. When the structures of the compounds with the highest correlation coefficients are evaluated, it is apparent that the structures are widely divergent. The compounds are commonly of natural product origin, have a high molecular weight, and are neutral or have a positive charge. The neutral compounds tend to be larger than the positively charged compounds. Negatively charged compounds were rare, comprising only 2% of the top 100 substrates. The finding in these studies that Pgp substrates tend to be larger and neutral or positively charged is consistent with results reported by others (33, 34).

Several fluorochromes are found among known Pgp substrates and among the top 100 compounds of the COMPARE list (Table 1). Olivomycin and chromomycin A3, among the top 100 compounds, have been previously described for use in fluorescence-activated cell-sorting analysis, although a lower wavelength is required for excitation than is used for the rhodamine assay (35). One compound, NSC 640085, was found

[4] Cell lines of the NCI drug screen are available upon request from Dr. Joe Mayo, National Cancer Institute, Fairview Center, Suite 205, Frederick, MD 21701–8527.

[5] A. T. Fojo, S. E. Bates, and M. Alvarez, unpublished observations.

[6] Questions regarding compounds emerging from the COMPARE analysis may be addressed to Dr. Ven Narayan, Drug Synthesis and Chemistry Branch, National Cancer Institute, EPN 833, 6130 Executive Blvd., Rockville, MD 20852. Questions regarding the COMPARE analysis should be addressed to Dr. Ken Paull, National Cancer Institute, EPN 811, 6130 Executive Blvd., Rockville, MD 20852.

to be fluorescent. Although significant drug efflux for NSC 640085 could not be shown, CsA enhanced its accumulation. This result suggests one of two possibilities; the first is that intracellular binding of NSC 640085 to a target is rapid and irreversible, so that Pgp must efflux the drug immediately, before it reaches the target, and the second is that, according to the hypothesis of Higgins and Gottesman (36), the cell membrane is cleared of some compounds, by Pgp, before they ever reach the cytoplasm.

The new drug screen of the NCI was established to allow rapid characterization of the cytotoxicity profiles of natural or synthetic compounds. One goal was to reduce the length of time required to determine whether a compound had promise as an anticancer agent. With the aid of the COMPARE analysis, the uniqueness of each tested compound can be evaluated. Thus, a tubulin-binding agent can be identified as distinct from an anthracycline (4). This allows selection of compounds with unique characteristics for further preclinical testing. This work adds another dimension to the screen, that of determining a mechanism of drug resistance for compounds by comparing cytotoxicity profiles with the profile of a drug resistance mechanism. Using the rhodamine efflux profile as a seed, 100 compounds with correlation coefficients of ≥ 0.816 were identified in the NCI database. When highly correlated compounds were in turn used as seeds for a search in the more limited "standard agent" database, an MDR profile was recognized. This profile included agents such as phyllanthoside, rubidazone, and homoharringtonine. This suggests that new compounds evaluated in the drug screen could be identified as Pgp substrates based on the results of the COMPARE analysis when the cytotoxicity data from each are used as a seed. The fact that the COMPARE analysis of an unknown compound generates an MDR profile may indicate that other mechanisms of resistance are less important than Pgp-mediated drug resistance.

The results also support an hypothesis generated in our laboratory studies involving regulation of Pgp function by phosphorylation. In these studies, increased transport of substrates was associated with poorer antagonistic properties (37), suggesting that Pgp antagonists are more poorly transported than the typical substrates. The COMPARE analysis for antagonists noted low correlation coefficients for rhodamine efflux, which suggests that Pgp binding, efflux blocking, and drug transport are separate entities. The r values for antagonists include those for verapamil ($r = -0.538$), CsA ($r = -0.164$), quinidine ($r = -0.376$), and tamoxifen ($r = 0.318$).

Determination that a compound is a Pgp substrate is of value in the clinical development of new drugs, in that single-agent trials in Pgp-expressing tumors are likely to result in failure. Although the incidence of expression remains unclear, in virtually every tumor type Pgp expression at some level has been reported (38). If the substrates identified with high correlation coefficients are transported to a greater degree than those substrates currently in clinical use, then a small amount of Pgp could confer resistance. This would result in failure of the compound to show activity in the clinical setting. Indeed, clinical studies with olivomycin and bisantrene were terminated after they failed to show activity. It is possible that the addition of a Pgp antagonist could prevent such resistance. Thus, early in its clinical development, a Pgp substrate could be combined with a Pgp antagonist. In fact, one could argue that such substrates should not be developed without the addition of a Pgp antagonist.

Acknowledgments

The authors would like to express their appreciation to Atwar Krishan, Antonieta Sauterig, and Larry Wellham for their advice in setting up FACScan analysis of drug accumulation, Eramus Schneider for help in setting up the PCR assay to measure MRP levels, Jon Ashwell for use of the Becton-Dickinson FACScan, and Kathleen Kocher for secretarial assistance.

References

1. Monks, A., D. Scudiero, P. Skehan, R. Shoemaker, K. Paull, D. Vistica, C. Hose, J. Langley, P. Cronise, A. Vaigro-Wolff, M. Gray-Goodrich, H. Campbell, J. Mayo, and M. Boyd. Feasibility of a high-flux anticancer drug screen using a diverse panel of cultured human tumor cell lines. *J. Natl. Cancer Inst.* **83**:757–766 (1991).
2. Paull, K. D., R. H. Shoemaker, L. Hodes, A. Monks, D. A. Scudiero, L. Rubinstein, J. Plowman, and M. R. Boyd. Display and analysis of patterns of differential activity of drugs against human tumor cell lines: development of mean graph and COMPARE algorithm. *J. Natl. Cancer Inst.* **81**:1088–1092 (1989).
3. Boyd, M. R., K. D. Paull, and L. R. Rubinstein. Data display and analysis strategies for the NCI disease oriented *in vitro* antitumor drug screen, in *Cytotoxic Anticancer Drugs: Models and Concepts for Drug Discovery and Development* (F. A. Valeriote, T. Korbit, and L. Baker, eds.). Kluwer Academic Publishers, Boston, 11–34 (1992).
4. Paull, K. D., E. Hamel, and L. Malspeis. Prediction of biochemical mechanisms of action from the *in vitro* antitumor screen of the National Cancer Institute, in *Cancer Chemotherapeutic Agents* (W. E. Foye, ed.). American Chemical Society, Washington, D. C. (in press).
5. Paull, K. D., C. M. Lin, L. Malspeis, and E. Hamel. Identification of novel antimitotic agents acting at the tubulin level by computer-assisted evaluation of differential cytotoxicity data. *Cancer Res.* **52**:3892–3900 (1992).
6. Van der Bliek, A. M., and P. Borst. Multidrug resistance. *Adv. Cancer Res.* **52**:165–203 (1989).
7. Pastan, I., and M. Gottesman. Multiple-drug resistance in human cancer. *N. Engl. J. Med.* **316**:1388–1393 (1987).
8. Arceci, R. J. Clinical significance of P-glycoprotein in multidrug resistance malignancies. *Blood* **81**:2215–2222 (1993).
9. Yagoda, A., G. Bosl, and H. Scher. Advances in chemotherapy, in *Recent Advances in Urologic Cancer* (N. Javadpour, ed.). Williams and Wilkins, Baltimore, 211–254 (1982).
10. Nadakavukaren, K. K., J. J. Nadakavukaren, and L. B. Chen. Increased rhodamine 123 uptake by carcinoma cells. *Cancer Res.* **45**:6093–6099 (1985).
11. Lampidis, T. J., S. D. Bernal, I. C. Summerhayes, and L. B. Chen. Selective toxicity of rhodamine 123 in carcinoma cells *in vitro*. *Cancer Res.* **43**:716–720 (1983).
12. Modica-Napolitano, J. S., and J. R. Aprille. Basis for the selective cytotoxicity of rhodamine 123. *Cancer Res.* **47**:4361–4365 (1987).
13. Efferth, T., H. Lohrke, and M. Volm. Reciprocal correlation between expression of P-glycoprotein and accumulation of rhodamine 123 in human tumors. *Anticancer Res.* **9**:1633–1638 (1989).
14. Bucana, C. D., R. Giavazzi, R. Nayar, C. A. O'Brian, C. Seid, L. E. Earnest, and D. Fan. Retention of vital dyes correlates inversely with the multidrug-resistant phenotype of Adriamycin-selected murine fibrosarcoma variants. *Exp. Cell Res.* **190**:69–75 (1990).
15. Coon, J. S., Y. Wang, S. D. Bines, P. N. Markham, A. S. F. Chong, and H. M. Gebel. Multidrug resistance activity in human lymphocytes. *Hum. Immunol.* **32**:134–140 (1991).
16. Chaudhary, P. M., and I. B. Roninson. Expression and activity of P-glycoprotein, a multidrug efflux pump, in human hematopoietic stem cells. *Cell* **66**:85–94 (1991).
17. Ludescher, C., J. Thaler, D. Drach, J. Drach, M. Spitaler, C. Gattringer, H. Huber, and J. Hofmann. Detection of activity of P-glycoprotein in human tumour samples using rhodamine 123. *Br. J. Haematol.* **82**:161–168 (1992).
18. Srour, E. F., T. Leemhuis, J. E. Brandt, K. van Besien, and R. Hoffman. Simultaneous use of rhodamine 123, phycoerythrin, Texas red, and allophycocyanin for the isolation of human hematopoietic progenitor cells. *Cytometry* **12**:179–183 (1991).
19. Krishan, A. Flow cytometric studies on intracellular drug fluorescence, in *Cell Cycle Analysis* (J. W. Gray and Z. Darzynkiewicz, eds.). Humana Press, Clifton, NJ, 337–347 (1986).
20. Bates, S. E., L. A. Mickley, Y.-N. Chen, N. Richert, J. Rudick, J. L. Biedler, and A. T. Fojo. Expression of a drug resistance gene in human neuroblastoma cell lines: modulation by retinoic acid-induced differentiation. *Mol. Cell. Biol.* **9**:4337–4344 (1989).
21. Mickley, L. A., S. E. Bates, N. D. Richert, S. Currier, S. Tanaka, F. Foss, N. Rosen, and A. T. Fojo. Modulation of the expression of a multidrug resistance gene (*mdr-1*/P-glycoprotein) by differentiating agents. *J. Biol. Chem.* **264**:18031–18040 (1989).
22. Chambers, T. C., E. M. McAvoy, J. W. Jacobs, and G. Eilon. Protein kinase C phosphorylates P-glycoprotein in multidrug resistant human KB carcinoma cells. *J. Biol. Chem.* **265**:7679–7686 (1990).

23. Bates, S. E., S. J. Currier, M. Alvarez, and A. T. Fojo. Modulation of P-glycoprotein phosphorylation and drug transport by sodium butyrate. *Biochemistry* **31**:6366–6372 (1992).
24. Lai, G.-M., Y.-N. Chen, L. A. Mickley, A. T. Fojo, and S. E. Bates. P-glycoprotein expression and schedule dependence of Adriamycin cytotoxicity in human colon carcinoma cell lines. *Int. J. Cancer* **49**:696–703 (1991).
25. Thomas, T. C., and M. G. McNamee. Purification of membrane protein. *Methods Enzymol.* **182**:499–520 (1990).
26. Tanaka, S., S. J. Currier, E. P. Bruggemann, K. Ueda, U. A. Germann, I. Pastan, and M. M. Gottesman. Use of recombinant P-glycoprotein fragments to produce antibodies to the multidrug transporter. *Biochem. Biophys. Res. Commun.* **166**:180–186 (1990).
27. Murphy, L. D., C. E. Herzog, J. B. Rudick, A. J. Fojo, and S. E. Bates. Use of the polymerase chain reaction in the quantitation of *mdr*-1 gene expression. *Biochemistry* **29**:10351–10356 (1990).
28. Skehan, P., R. Storeng, D. Scudiero, A. Monks, J. McMahon, D. Vistica, J. T. Warren, H. Bokesch, S. Kenney, and M. R. Boyd. New colorimetric cytotoxicty assay for anticancer-drug screening. *J. Natl. Cancer Inst.* **82**:1107–1112 (1990).
29. Herzog, C. E., J. B. Trepel, L. A. Mickley, S. E. Bates, and A. T. Fojo. Various methods of analysis of *mdr-1*/P-glycoprotein in human colon cancer cell lines. *J. Natl. Cancer Inst.* **84**:711–716 (1992).
30. Cole, S. P. C., G. Bhardwaj, J. H. Gerlach, J. E. Mackie, C. E. Grant, K. C. Almquist, A. J. Stewart, E. U. Kurz, A. M. V. Duncan, and R. G. Deeley. Overexpression of a transporter gene in a multidrug-resistant human lung cancer cell line. *Science (Washington D. C.)* **258**:1650–1654 (1993).
31. Berman, E., M. Adams, R. Duigou-Osterndorf, L. Godfrey, B. Clarkson, and M. Andreeff. Effect of tamoxifen on cell lines displaying the multidrug-resistant phenotype. *Blood* **77**:818–825 (1991).
32. Bates, S. E., C. Y. Shieh, L. A. Mickley, H. L. Dichek, A. Gazdar, D. L. Loriaux, and A. T. Fojo. Mitotane enhances cytotoxicity of chemotherapy in cell lines expressing a multidrug resistance gene (*mdr*-1/P-glycoprotein) which is also expressed by adrenocortical carcinomas. *J. Clin. Endocrinol. Metab.* **73**:18–29 (1991).
33. Zamora, J. M., H. L. Pearce, and W. T. Beck. Physical-chemical properties shared by compounds that modulate multidrug resistance in human leukemia cells. *Mol. Pharmacol.* **33**:454–462 (1988).
34. Ford, J. M., W. C. Prozialeck, and W. N. Hait. Structural features determining activity of phenothiazines and related drugs for inhibition of cell growth and reversal of multidrug resistance. *Mol. Pharmacol.* **35**:105–115 (1989).
35. Crissman, H. A., and R. A. Tobey. Specific staining of DNA with the fluorescent antibiotics, mithramycin, chromomycin, and olivomycin. *Methods Cell Biol.* **33**:97–103 (1990).
36. Higgins, C. F., and M. M. Gottesman. Is the multidrug transporter a flippase? *Trends Biochem. Sci.* **17**:18–21 (1992).
37. Bates, S. E., J. S. Lee, B. Dickstein, M. Spolyar, and A. T. Fojo. Differential modulation of P-glycoprotein transport by protein kinase inhibition. *Biochemistry* **32**:9156–9164 (1993).
38. Goldstein, L. J., H. Galski, A. Fojo, M. Willingham, S. L. Lai, A. Gazder, R. Pirker, A. Green, W. Crist, G. M. Brodeur, M. Lieber, J. Cossman, M. M. Gottesman, and I. Pastan. Expression of a multidrug resistance gene in human cancers. *J. Natl. Cancer Inst.* **81**:116–124 (1989).

Send reprint requests to: Susan E. Bates, Building 10, Room 12N226, 9000 Rockville Pike, Bethesda, MD 20892.